Acta Crystallographica Section F
Structural Biology and Crystallization Communications
ISSN 1744-3091

Purification, crystallization and preliminary X-ray diffraction analysis of the IL-20–IL-20R1–IL-20R2 complex

Naomi J. Logsdon,[a] Christopher E. Allen,[a] Kanagalaghatta R. Rajashankar[b] and Mark R. Walter[a,c]*

[a]Center for Biophysical Sciences and Engineering, University of Alabama at Birmingham, Birmingham, AL 35294, USA, [b]NE-CAT/Cornell University, Argonne, IL 60439, USA, and [c]Department of Microbiology, University of Alabama at Birmingham, Birmingham, AL 35294, USA

Correspondence e-mail: walter@uab.edu

Received 16 September 2011
Accepted 19 November 2011

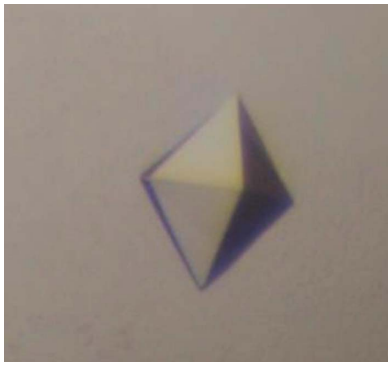

Interleukin-20 (IL-20) is an IL-10-family cytokine that regulates innate and adaptive immunity in skin and other tissues. In addition to protecting the host from various external pathogens, dysregulated IL-20 signaling has been shown to contribute to the pathogenesis of human psoriasis. IL-20 signals through two cell-surface receptor heterodimers, IL-20R1–IL-20R2 and IL-22R1–IL-20R2. In this report, crystals of the IL-20–IL-20R1–IL-20R2 ternary complex have been grown from polyethylene glycol solutions. The crystals belonged to space group $P4_12_12$ or $P4_32_12$, with unit-cell parameters a = 111, c = 135 Å, and diffracted X-rays to 3 Å resolution. The crystallographic asymmetric unit contains one IL-20–IL-20R1–IL-20R2 complex, corresponding to a solvent content of approximately 54%.

1. Introduction

Interleukin-20 (IL-20) is an α-helical cytokine that was first identified by computational sequence searches of a human keratinocyte library (Blumberg *et al.*, 2001). Further analysis revealed that IL-20 is a member of the IL-10 family of cytokines that includes IL-10, IL-19, IL-22, IL-24 and IL-26 (Ouyang *et al.*, 2011; Zdanov, 2010; Pestka *et al.*, 2004). The biological functions of IL-20 are still being defined. However, overexpression of IL-20 in transgenic mice caused skin abnormalities that resemble the pathogenesis of human psoriasis (Blumberg *et al.*, 2001). Consistent with this observation, IL-20 prevents the terminal differentiation of keratinocytes and upregulates antimicrobial peptides to protect epithelial surfaces from invading pathogens (Sa *et al.*, 2007). Interestingly, these functions are very similar to those of IL-22, which has also been shown to induce expression of IL-20 (Wolk *et al.*, 2009). Characterization of psoriasis patient samples has shown that IL-22 and IL-20 blood levels correlate with the significance of disease (Wolk *et al.*, 2009). Based on these data, IL-20 is proposed to extend and exacerbate psoriatic skin inflammation initiated by IL-22 and other early immune events (Sabat & Wolk, 2011).

In addition to psoriasis, IL-20 has been linked to other pathologies and biological functions. In particular, IL-20 is upregulated in samples derived from synovial membranes of rheumatoid arthritis patients compared with healthy controls (Hsu *et al.*, 2006). Additional studies revealed that antibody-mediated neutralization of IL-20 activity inhibited inflammation and bone loss in an experimental arthritis model (Hsu & Chang, 2010). IL-20 is also overexpressed in endothelial cells of human atherosclerotic arteries, which was further confirmed in a mouse model of atherosclerosis (Chen *et al.*, 2006). IL-20 may be both protective against and contribute to inflammation in atherosclerosis. Firstly, IL-20 appears to be upregulated under hypoxic conditions and has been shown to promote angiogenesis (Chen *et al.*, 2006; Hsieh *et al.*, 2006; Tritsaris *et al.*, 2007). In addition, IL-20 upregulates the production of the chemokines MIG and I-TAC, which recruit inflammatory cells into the damaged areas (Chen *et al.*, 2006).

IL-20 biological responses are mediated through two heterodimeric receptor complexes consisting of the IL-20R1–IL-20R2 and IL-22R1–IL-20R2 receptor chains (Dumoutier *et al.*, 2001; Parrish-

Novak *et al.*, 2002). IL-19, IL-20 and IL-24 all signal through the IL-20R1–IL-20R2 heterodimer, while IL-20 and IL-24 can also signal through the IL-22R1–IL-20R2 complex (Dumoutier *et al.*, 2001; Parrish-Novak *et al.*, 2002). In addition, IL-22R1 pairs with the IL-10R2 chain to induce IL-22 signaling (Xie *et al.*, 2000; Kotenko *et al.*, 2001). Characterization of receptor expression demonstrates that IL-20R1, IL-20R2 and IL-22R1 are selectively expressed on epithelial/stromal cells (Wolk *et al.*, 2002; Nagalakshmi *et al.*, 2004). Selective receptor expression provides a mechanism to target IL-20 to epithelial surfaces from the many cellular sources of IL-20, which include keratinocytes, monocytes and endothelial and dendritic cells (Wegenka, 2010).

The structural mechanisms that control IL-20 receptor sharing and the complex biology of IL-10-family cytokines are just beginning to be unraveled (Wegenka, 2010; Ouyang *et al.*, 2011; Gallagher, 2010; Zdanov, 2010). At this time, structures of the IL-10–IL-10R1 (Jones *et al.*, 2002; Josephson, Logsdon *et al.*, 2001; Yoon *et al.*, 2005), IL-22–IL-22R1 (Jones *et al.*, 2008; Bleicher *et al.*, 2008) and IL-29–IL-28R1 (Miknis *et al.*, 2010) binary complexes have been defined. However, the structure of a fully assembled ternary complex containing an R2 chain has not been reported. To address this problem, we have crystallized the IL-20–IL-20R1–IL-20R2 ternary complex for structural studies. The structure of the complex should provide the molecular basis for receptor promiscuity of IL-20R2-binding cytokines and potentially assist in the design of novel antagonists to treat IL-20-mediated disease.

2. Materials and methods

2.1. Cloning, expression and purification

Restriction enzymes were purchased from New England Biolabs. All PCR experiments were performed using *Pfu* polymerase (Stratagene). An IL-20 expression construct was created by amplifying IL-20 residues 25–176 (UniProt Q9NYY1) from cDNA obtained from the Harvard Institute of Proteomics. The N-terminus of IL-20 was modified to code for a six-histidine affinity tag followed by a factor Xa protease site. The amplified PCR product was cut and ligated into the pMT/V5-HisA expression plasmid (Invitrogen) to form pAHF-IL-20. The mature IL-20 peptide sequence was also cloned into pET32 using *Nde*I and *Xho*I to generate pET32-IL-20 for bacterial expression.

PCR was also performed using templates for IL-20R1 (IMAGE clone ID 2700520) and IL-20R2 to generate the extracellular receptor fragments followed by a C-terminal factor Xa protease site and six-histidine tag. DNA corresponding to IL-20R1 residues 29–245 (UniProt Q9UHF4) and IL-20R2 residues 30–231 (UniProt Q6UXL0) were amplified and inserted into the pMT/V5-HisA expression plasmid (Invitrogen) to form pMT-IL-20R1 and pMT-IL-20R2. Site-directed mutagenesis was used to remove the two glycosylation sites in IL-20R2 by mutating Asn40 and Asn134 to glutamines (IL-20R2^{QQ}) using the QuikChange mutagenesis kit (Stratagene).

Transfection and selection of *Drosophila* S2 cells with pAHF-IL-20, pMTA-IL-20R1 or pMTA-IL-20R2^{QQ} plus the hygromycin-resistance vector (pHYGRO) were performed as suggested by the manufacturer (Invitrogen). Expression was induced at a cell density of 5×10^6 cells ml^{-1} by the addition of 200 m*M* Cu_2SO_4 (0.5 m*M* final concentration) and allowed to proceed for 5 d. Purification of IL-20, IL-20R1 and IL-20R2^{QQ} were all performed using the same protocol. Briefly, cells were removed by centrifugation and the expression medium was dialyzed into buffer consisting of 20 m*M* Tris–HCl pH 7.9, 0.5 *M* NaCl (buffer *A*) that contained 5.0 m*M* imidazole. 1 l dialyzed medium for each protein was subsequently applied onto a 10 ml nickel-affinity column (Novagen). The proteins were extensively washed in buffer *A* containing 20 m*M* imidazole and subsequently eluted with a 1 *M* imidazole step gradient. Eluted fractions containing each protein were dialyzed overnight into 20 m*M* Tris–HCl pH 8.0, 150 m*M* NaCl.

For selenomethionine labeling of IL-20, pET32-IL-20 was transformed into *Escherichia coli* B834 pRare2 cells, a methionine auxotroph, for expression. 5 ml overnight culture grown in Luria–Bertani medium supplemented with 100 µg ml^{-1} carbenicillin and 34 µg ml^{-1} chloramphenicol was used to inoculate 1 l M9 SeMet high-yield medium (Medicilon). Cells were grown at 310 K to an optical density of 0.9 (600 nm) and IL-20 expression was induced by addition of 1 m*M* IPTG for 20 h. SeMet-IL-20 (IL-20^{SeMet}) was expressed in inclusion bodies (IBs) that were purified by sonication in 100 m*M* Tris–HCl, 100 m*M* NaCl, 5 m*M* EDTA, 0.1 *M* phenylmethylsulfonyl fluoride pH 8. The IBs were solubilized in 6 *M* guanidine–HCl, 5 m*M* DTT. Refolding of IL-20^{SeMet} was initiated by tenfold dilution of solubilized IL-20^{SeMet} into a refolding buffer consisting of 100 m*M* Tris pH 8.0, 50 m*M* NaCl, 2.5 m*M* EDTA, 2 m*M* reduced glutathione, 0.2 m*M* oxidized glutathione and 600 m*M* arginine. Purification of the refolded material was performed by sequential ion-exchange chromatography using HS20 and HQ20 media (Perseptive Biosystems) followed by gel-filtration chromatography (GE Healthcare).

Protein concentration was determined by UV absorbance at 280 nm to obtain concentrations in mg ml^{-1} using calculated $\varepsilon^{0.1\%}$ values of 0.655, 1.91 and 1.53 for IL-20, IL-20R1 and IL-20R2, respectively. Ternary complexes were formed by mixing IL-20 or IL-20^{SeMet} with IL-20R1 and IL-20R2 in a 1:1:1 molar ratio with factor Xa [1:50(*w*:*w*) ratio] in 20 m*M* Tris–HCl pH 8.0, 150 m*M* NaCl, 2 m*M* $CaCl_2$. The resulting digestion mixture was concentrated using a Centriprep 10 (Amicon) and injected onto a gel-filtration column (GE Healthcare) equilibrated in 20 m*M* Tris–HCl pH 8.0 and 150 m*M* NaCl. Fractions containing IL-20–IL-20R1–IL-20R2 complexes were concentrated to ~7 mg ml^{-1} for crystallization studies.

2.2. Crystallization

All crystallization experiments employed the hanging-drop method performed in 24-well Linbro plates (Hampton Research). Crystallization drops consisted of 1 µl IL-20–IL-20R1–IL-20R2^{QQ} or IL-20^{SeMet}–IL-20R1–IL-20R2^{QQ} complex at 7.5 mg ml^{-1} in 20 m*M* Tris–HCl pH 8.0, 150 m*M* NaCl combined with 1 µl well solution. The drops (2 µl) were equilibrated over 699 µl well solution at 298 K.

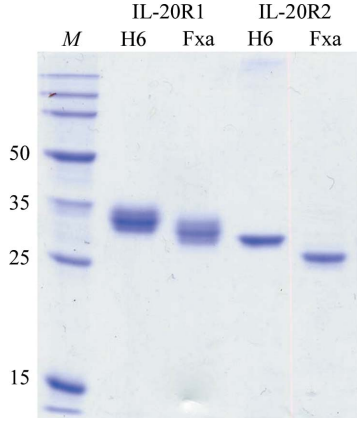

Figure 1
SDS–PAGE gel of purified IL-20R1 and IL-20R2^{QQ}. Gel lanes show the receptors before (H6) and after (Fxa) cleavage with factor Xa protease. Molecular-weight markers (*M*) are shown together with the sizes (in kDa) of specific bands.

3. Results and discussion

3.1. IL-20 forms a stable ternary complex with IL-20R1 and IL-20R2^{QQ}

The extracellular ligand-binding domains of IL-20R1 and IL-20R2 contain six and two N-linked (N*X*S/T, where *X* is any amino acid) glycosylation sites, respectively. As a result, IL-20R1 appears as a broad band when run on an SDS–PAGE gel (Fig. 1). Because IL-20R2 contained only two N-linked carbohydrate-attachment sites (Asn40 and Asn134), the residues were mutated to glutamine (IL-20R2^{QQ}) to improve crystal formation, as previously observed for the IL-10–IL-10R1 binary complex (Josephson, McPherson *et al.*, 2001). As a result, IL-20R2^{QQ} runs as a sharp band on SDS–PAGE gels (Fig. 1). Consistent with previous studies (Pletnev *et al.*, 2003), mixing IL-20 or IL-20^{SeMet} with IL-20R1 and IL-20R2 in a 1:1.2:1.2 molar ratio resulted in the formation of a stable ternary complex which could be separated from excess receptor components by gel-filtration chromatography (Fig. 2). IL-20 does not contain any N-linked glycosylation sites and IL-20 and IL-20^{SeMet} complexes were indistinguishable when analyzed by size-exclusion chromatography.

3.2. Crystallization

Initial crystal screening experiments were performed using complexes containing '*Drosophila*-produced' IL-20 (IL20^{Dros}) (IL-20^{Dros}–IL-20R1–IL-20R2). Crystallization screens performed using Crystal Screen (Hampton Research) at 298 K yielded microcrystals (∼5 µm) in condition No. 22, which consisted of 0.2 *M* sodium acetate trihydrate, 30% PEG 4000, 0.1 *M* Tris–HCl pH 8.5. The initial conditions were optimized using a streak-seeding procedure in drops containing 0.3 *M* sodium acetate, Tris pH 8.5, 13% PEG 4000. After 2 h, the drops were streaked with crushed microcrystals from experiments using condition No. 22. This procedure resulted in the formation of tetragonal bipyramids with dimensions of ∼100–150 µm on each edge (Fig. 3*a*). Several crystals were removed from the crystallization drops, washed extensively in well solution and then subjected to SDS–PAGE analysis. As shown in Fig. 3(*b*), this analysis confirmed the presence of each component of the IL-20–IL-20R1–IL-20R2 complex in the crystals.

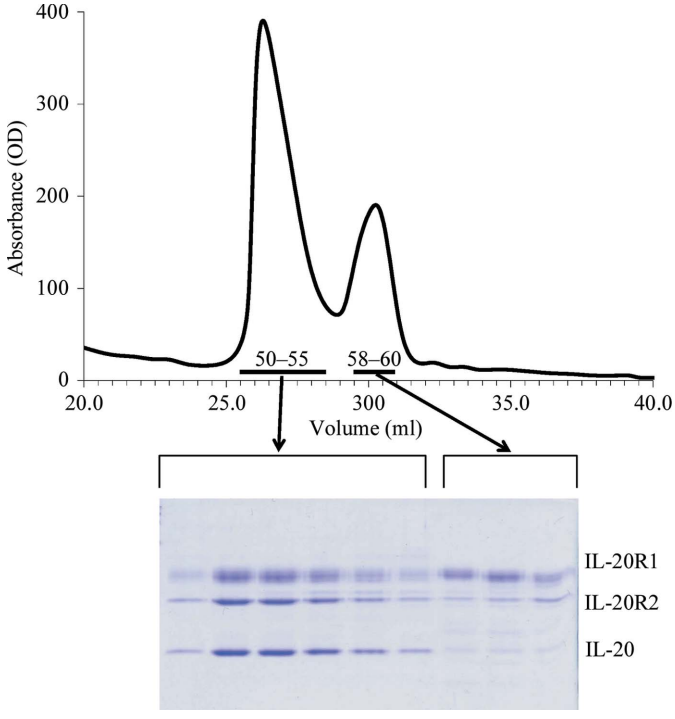

Figure 2
Gel filtration of the IL-20^{SeMet}–IL-20R1–IL-20R2^{QQ} ternary complex. The top panel shows the chromatogram of the ternary complex (fractions 50–55) and an excess of free receptors (fractions 58–60). The SDS–PAGE gel in the bottom panel shows the composition of the fractions eluting from the column.

Table 1
Data-collection statistics.

Values in parentheses are for the highest resolution shell.

Wavelength (Å)	0.97918
Resolution (Å)	50–3.0 (3.11–3.00)
No. of observations	239380
No. of unique observations	32340
Multiplicity	7.4 (7.1)
Completeness (%)	100.0 (100.0)
$\langle I/\sigma(I)\rangle$	20.7 (2.3)
R_{merge} (%)	11.9 (85.3)
Space group	$P4_12_12/P4_32_12$
Unit-cell parameters	
a (Å)	111
c (Å)	135

3.3. X-ray diffraction

Crystals of IL-20^{Dros}–IL-20R1–IL-20R2 were flash-cooled for low-temperature data collection in a nitrogen stream (100 K) following exchange of the drop solution with a solution consisting of 0.1 *M* Tris–HCl pH 8.5, 0.3 *M* ammonium acetate, 17% PEG 4000, 15% glycerol. The crystals exhibited highly variable diffraction, with the best crystals diffracting to 4 Å resolution. Continued screening of crystallization conditions, additives and annealing procedures did not further improve diffraction.

Based on this result, we sought to obtain independent phase information on the complex to assist in solving the low-resolution structure. To accomplish this, we expressed IL-20^{SeMet}, which contains three methionines. Although IL-20^{SeMet}–IL-20R1–IL-20R2 behaved the same as the IL-20^{Dros} ternary complex during purification, it behaved differently during crystallization. In particular, the IL-20^{SeMet}–IL-20R1–IL-20R2 complex yielded 100–200 µm crystals under the same conditions as the IL-20^{Dros}–IL-20R1–IL-20R2 complex without streak-seeding. IL-20^{SeMet}-containing ternary-complex crystals also showed variable diffraction. However, diffraction quality was better as screening revealed two crystals that diffracted to ∼3.2 Å resolution on a home source.

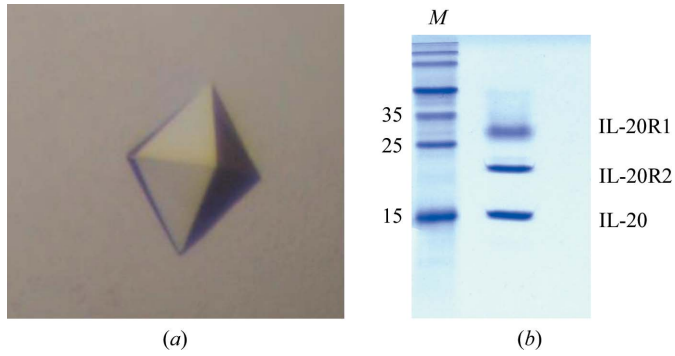

Figure 3
(*a*) Crystal of the IL-20^{SeMet}–IL-20R1–IL-20R2^{QQ} complex. The crystal shown is approximately 75 µm wide and 150 µm long. The composition of the crystals was determined by extensive washing of four crystals, followed by analysis by SDS–PAGE (*b*). Molecular-weight markers (lane *M*) are shown together with the sizes (in kDa) of specific bands.

Single-wavelength anomalous diffraction (SAD) data were collected from these crystals on the North Eastern Collaborative Access Team (NE-CAT) beamline 24-ID-C at the Advanced Photon Source, Argonne National Laboratory. A complete data set was collected to ∼3 Å resolution using an ADSC Q315 CCD detector and a wavelength of 0.97918 Å. Reflection intensities were indexed, integrated and scaled using *HKL*-2000 (Otwinowski & Minor, 1997). The space group was identified as either $P4_12_12$ or $P4_32_12$, with unit-cell parameters a = 111, c = 135 Å. This was accomplished using the *HKL*-2000 indexing routine, analysis of merging statistics and analysis of systematic absences to define the crystal lattice, Laue group and space group, respectively. Data-collection statistics are shown in Table 1. No evidence of twinning was observed when analyzing *L*-test (Padilla & Yeates, 2003) and cumulative intensity statistics in *CTRUNCATE* within the *CCP*4 package (v.6.1.13; Winn *et al.*, 2011).

Based on the molecular weights of IL-20 (molecular weight 17 769 Da), IL-20R1 (molecular weight ∼33 500 Da) and IL-20R2 (molecular weight 26 481 Da), the molecular weight of the IL-20–IL-20R1–IL-20R2 complex is 77 750 Da. Calculations using this molecular weight resulted in one reasonable solvent estimate of 54% (V_M = 2.68 Å^3 Da^{-1}), corresponding to one IL-20–IL-20R1–IL-20R2 complex in the asymmetric unit (Matthews, 1968). Solving the positions of the heavy-atom substructure, model building and refinement are currently under way.

This work was supported by the NIH (grants AI47300 and AI47300-S1). Use of the Advanced Photon Source was supported by the US Department of Energy, Office of Science, Office of Basic Energy Sciences under Contract No. W-31-109-Eng-38. We thank Jean-Christophe Renauld for IL-20R2 cDNA and Joshua LaBaer, Institute of Proteomics, Harvard Medical School for IL-20 cDNA. Work conducted at the APS North Eastern Collaborative Access Team (NE-CAT) beamline is supported by award RR-15301 from the National Center for Research Resources at the NIH and DOE/OBES Contract No. DE-AC02-06CH11357.

References

Bleicher, L., de Moura, P. R., Watanabe, L., Colau, D., Dumoutier, L., Renauld, J.-C. & Polikarpov, I. (2008). *FEBS Lett.* **582**, 2985–2992.
Blumberg, H. *et al.* (2001). *Cell*, **104**, 9–19.
Chen, W.-Y., Cheng, B.-C., Jiang, M.-J., Hsieh, M.-Y. & Chang, M.-S. (2006). *Arterioscler. Thromb. Vasc. Biol.* **26**, 2090–2095.
Dumoutier, L., Leemans, C., Lejeune, D., Kotenko, S. V. & Renauld, J.-C. (2001). *J. Immunol.* **167**, 3545–3549.
Gallagher, G. (2010). *Cytokine Growth Factor Rev.* **21**, 345–352.
Hsieh, M.-Y., Chen, W.-Y., Jiang, M.-J., Cheng, B.-C., Huang, T.-Y. & Chang, M.-S. (2006). *Genes Immun.* **7**, 234–242.
Hsu, Y.-H. & Chang, M.-S. (2010). *Arthritis Rheum.* **62**, 3311–3321.
Hsu, Y.-H., Li, H.-H., Hsieh, M.-Y., Liu, M.-F., Huang, K.-Y., Chin, L.-S., Chen, P.-C., Cheng, H.-H. & Chang, M.-S. (2006). *Arthritis Rheum.* **54**, 2722–2733.
Jones, B. C., Logsdon, N. J., Josephson, K., Cook, J., Barry, P. A. & Walter, M. R. (2002). *Proc. Natl Acad. Sci. USA*, **99**, 9404–9409.
Jones, B. C., Logsdon, N. J. & Walter, M. R. (2008). *Structure*, **16**, 1333–1344.
Josephson, K., Logsdon, N. J. & Walter, M. R. (2001). *Immunity*, **15**, 35–46.
Josephson, K., McPherson, D. T. & Walter, M. R. (2001). *Acta Cryst.* D**57**, 1908–1911.
Kotenko, S. V., Izotova, L. S., Mirochnitchenko, O. V., Esterova, E., Dickensheets, H., Donnelly, R. P. & Pestka, S. (2001). *J. Biol. Chem.* **276**, 2725–2732.
Matthews, B. W. (1968). *J. Mol. Biol.* **33**, 491–497.
Miknis, Z. J., Magracheva, E., Li, W., Zdanov, A., Kotenko, S. V. & Wlodawer, A. (2010). *J. Mol. Biol.* **404**, 650–664.
Nagalakshmi, M. L., Murphy, E., McClanahan, T. & de Waal Malefyt, R. (2004). *Int. Immunopharmacol.* **4**, 577–592.
Otwinowski, Z. & Minor, W. (1997). *Methods Enzymol.* **276**, 307–326.
Ouyang, W., Rutz, S., Crellin, N. K., Valdez, P. A. & Hymowitz, S. G. (2011). *Annu. Rev. Immunol.* **29**, 71–109.
Padilla, J. E. & Yeates, T. O. (2003). *Acta Cryst.* D**59**, 1124–1130.
Parrish-Novak, J., Xu, W., Brender, T., Yao, L., Jones, C., West, J., Brandt, C., Jelinek, L., Madden, K., McKernan, P. A., Foster, D. C., Jaspers, S. & Chandrasekher, Y. A. (2002). *J. Biol. Chem.* **277**, 47517–47523.
Pestka, S., Krause, C. D., Sarkar, D., Walter, M. R., Shi, Y. & Fisher, P. B. (2004). *Annu. Rev. Immunol.* **22**, 929–979.
Pletnev, S., Magracheva, E., Kozlov, S., Tobin, G., Kotenko, S. V., Wlodawer, A. & Zdanov, A. (2003). *Biochemistry*, **42**, 12617–12624.
Sa, S. M., Valdez, P. A., Wu, J., Jung, K., Zhong, F., Hall, L., Kasman, I., Winer, J., Modrusan, Z., Danilenko, D. M. & Ouyang, W. (2007). *J. Immunol.* **178**, 2229–2240.
Sabat, R. & Wolk, K. (2011). *J. Dtsch Dermatol. Ges.* **9**, 518–523.
Tritsaris, K., Myren, M., Ditlev, S. B., Hübschmann, M. V., van der Blom, I., Hansen, A. J., Olsen, U. B., Cao, R., Zhang, J., Jia, T., Wahlberg, E., Dissing, S. & Cao, Y. (2007). *Proc. Natl Acad. Sci. USA*, **104**, 15364–15369.
Wegenka, U. M. (2010). *Cytokine Growth Factor Rev.* **21**, 353–363.
Winn, M. D. *et al.* (2011). *Acta Cryst.* D**67**, 235–242.
Wolk, K., Kunz, S., Asadullah, K. & Sabat, R. (2002). *J. Immunol.* **168**, 5397–5402.
Wolk, K., Witte, E., Warszawska, K., Schulze-Tanzil, G., Witte, K., Philipp, S., Kunz, S., Döcke, W. D., Asadullah, K., Volk, H. D., Sterry, W. & Sabat, R. (2009). *Eur. J. Immunol.* **39**, 3570–3581.
Xie, M.-H., Aggarwal, S., Ho, W.-H., Foster, J., Zhang, Z., Stinson, J., Wood, W. I., Goddard, A. D. & Gurney, A. L. (2000). *J. Biol. Chem.* **275**, 31335–31339.
Yoon, S. I., Jones, B. C., Logsdon, N. J. & Walter, M. R. (2005). *Structure*, **13**, 551–564.
Zdanov, A. (2010). *Cytokine Growth Factor Rev.* **21**, 325–330.